

High-fidelity transmission of sensory information by single cerebellar mossy fibre boutons

Ede A. Rancz^{1*}, Taro Ishikawa^{1*}, Ian Duguid^{1*}, Paul Chadderton^{1*}, Séverine Mahon¹ & Michael Häusser¹

Understanding the transmission of sensory information at individual synaptic connections requires knowledge of the properties of presynaptic terminals and their patterns of firing evoked by sensory stimuli. Such information has been difficult to obtain because of the small size and inaccessibility of nerve terminals in the central nervous system. Here we show, by making direct patch-clamp recordings *in vivo* from cerebellar mossy fibre boutons—the primary source of synaptic input to the cerebellar cortex^{1,2}—that sensory stimulation can produce bursts of spikes in single boutons at very high instantaneous firing frequencies (more than 700 Hz). We show that the mossy fibre–granule cell synapse exhibits high-fidelity transmission at these frequencies, indicating that the rapid burst of excitatory postsynaptic currents underlying the sensory-evoked response of granule cells³ can be driven by such a presynaptic spike burst. We also demonstrate that a single mossy fibre can trigger action potential bursts in granule cells *in vitro* when driven with *in vivo* firing patterns. These findings suggest that the relay from mossy fibre to granule cell can act in a ‘detonator’ fashion, such that a single presynaptic afferent may be sufficient to transmit the sensory message. This endows the cerebellar mossy fibre system with remarkable sensitivity and high fidelity in the transmission of sensory information.

We have used a parallel approach to make patch-clamp recordings from cerebellar mossy fibre boutons both *in vivo* and *in vitro*. In cerebellar slices, we targeted patch-clamp recordings to small structures (diameter about 2–3 µm) visible among the granule cells. Biocytin filling and subsequent processing (Fig. 1a; $n = 12$) confirmed their identity as mossy fibre boutons, revealing characteristic thorny excrescences on collaterals of a thin axon emerging from the white matter^{1,2}. Mossy fibre boutons had a distinctive set of electrophysiological characteristics, including an absence of spontaneous synaptic potentials or currents, a small membrane capacitance ($C_m = 1.81 \pm 0.46$ pF (mean \pm s.e.m.), $n = 7$; Supplementary Fig. 2), a high input resistance ($R_{\text{input}} = 520 \pm 88$ MΩ, $n = 12$), pronounced outward rectification, and time-dependent ‘sag’ on hyperpolarization (Fig. 1c). Using patch pipettes of similar tip sizes and geometries, we made recordings from mossy fibre boutons in the granule cell layer of cerebellar cortex *in vivo*, identified on the basis of their subthreshold and suprathreshold electrophysiological properties (Supplementary Table 1), which were identical with those observed *in vitro*. Mossy fibre boutons *in vivo* showed no detectable spontaneous synaptic events (Supplementary Fig. 3) and, when recovered, had a similar morphology (Fig. 1b) to those *in vitro*.

Mossy fibre boutons *in vivo* fired action potentials spontaneously at a rate of 3.9 ± 0.8 Hz ($n = 10$; Fig. 1d), distinct from the spontaneous firing rates of interneurons in the granule cell layer and of granule cells *in vivo*^{3–5}. Strong hyperpolarization of mossy fibre boutons (below -90 mV) or voltage clamp (at -90 mV) did not prevent

spontaneous firing ($n = 5$), suggesting that action potential initiation occurred electrotonically distant from the site of recording. However, action potential amplitude showed a marked dependence on membrane potential, decreasing with depolarization (Fig. 1g, h), consistent with local Na^+ -channel inactivation limiting active invasion of the bouton at depolarized membrane potentials^{6,7}. Previous extracellular recordings from putative mossy fibre units *in vivo* have reported firing rates of up to 1 kHz (refs 8–11). To determine the firing rates that single mossy fibre boutons can sustain, we injected brief current pulses to generate action potentials. Whereas long step-current injections produced only a single action potential (Fig. 1c, d), the injection of brief current pulses at high frequency resulted in repetitive firing at 500 Hz or greater (Fig. 1e, f; $n = 6$). These data indicate that cerebellar mossy fibres are capable of faithfully generating spikes at extremely high frequencies.

Spiking evoked by peripheral sensory stimulation was observed in both cell-attached and subsequent whole-cell recordings from mossy fibre boutons. Sensory stimulation reliably generated bursts of spikes (4.2 ± 0.6 action potentials with an average inter-spike interval (ISI) of 12.4 ± 1.7 ms; $n = 3$ responding boutons out of 10 boutons tested; Fig. 2a–c). The onset latency of spiking was 27.0 ± 19.2 ms, consistent with the onset latency of granule-cell excitatory postsynaptic currents (EPSCs) with the same stimulus and presumably reflecting a mixture of direct trigeminocerebellar and corticopontine input¹². During the sensory-evoked presynaptic burst, the waveform of the action potential remained relatively constant, with the amplitude and maximal rate of rise decreasing by $15.3 \pm 10.3\%$ ($P > 0.1$) and $24.7 \pm 8.4\%$ ($P < 0.05$), respectively, within the burst, and with spike width increasing by only $4.9 \pm 2.7\%$ ($0.05 < P < 0.1$).

Sensory stimulation evokes a burst of EPSCs in cerebellar granule cells³, the primary synaptic target of cerebellar mossy fibres. Because each granule cell receives only a small number of mossy fibre inputs, we determined whether transmission through a single mossy fibre could account for the postsynaptic burst (Supplementary Fig. 1) by comparing the dynamics of sensory-evoked presynaptic and postsynaptic responses. First, the number of sensory-evoked postsynaptic EPSCs (5.4 ± 0.7 , $n = 14$; Fig. 2d, e) was indistinguishable from the number of sensory-evoked spikes in single presynaptic mossy fibre boutons ($P = 0.45$). Second, the latency of the first sensory-evoked presynaptic spike was similar to that of the first sensory-evoked EPSC (16.8 ± 1.9 ms, $P = 0.26$), and the timing of individual spikes was highly irregular (the coefficient of variation of evoked action potential intervals was 1.00 ± 0.06 ; Fig. 2c), comparable to the coefficient of variation of evoked postsynaptic EPSCs (0.69 ± 0.03 , $n = 14$; Fig. 2d). Third, the minimum ISI of sensory-evoked action potentials was short (1.9 ± 0.5 ms, $n = 3$; Fig. 2b, e) and not significantly different from the minimum inter-event intervals (IEIs) of the postsynaptic EPSCs (3.1 ± 0.5 ms, $P = 0.27$; Fig. 2e). Finally, the mean ISI

¹Wolfson Institute for Biomedical Research and Department of Physiology, University College London, Gower Street, London WC1E 6BT, UK.

*These authors contributed equally to this work.

of the presynaptic spikes was also not different from the mean IEI (13.5 ± 1.0 ms, $P = 0.64$; Fig. 2e). Because the number, pattern and frequency of sensory-evoked EPSCs were indistinguishable from those of the spikes in the sensory-evoked presynaptic spike burst, our findings are consistent with the idea that a single mossy fibre could provide the synaptic input observed in granule cells during sensory stimulation.

To further understand information transmission at the mossy fibre–granule cell synapse, we compared synaptic properties *in vivo* with those *in vitro*. We activated single mossy fibre–granule cell inputs using minimal stimulation in cerebellar slices¹³ (Supplementary Fig. 4). Given the uncertainty about the extracellular calcium concentration ($[Ca^{2+}]_e$) *in vivo*^{14,15} and the sensitivity of neurotransmitter release probability to $[Ca^{2+}]_e$, we compared EPSC amplitudes and paired-pulse ratios in the presence of 1.2 or 2 mM $[Ca^{2+}]_e$

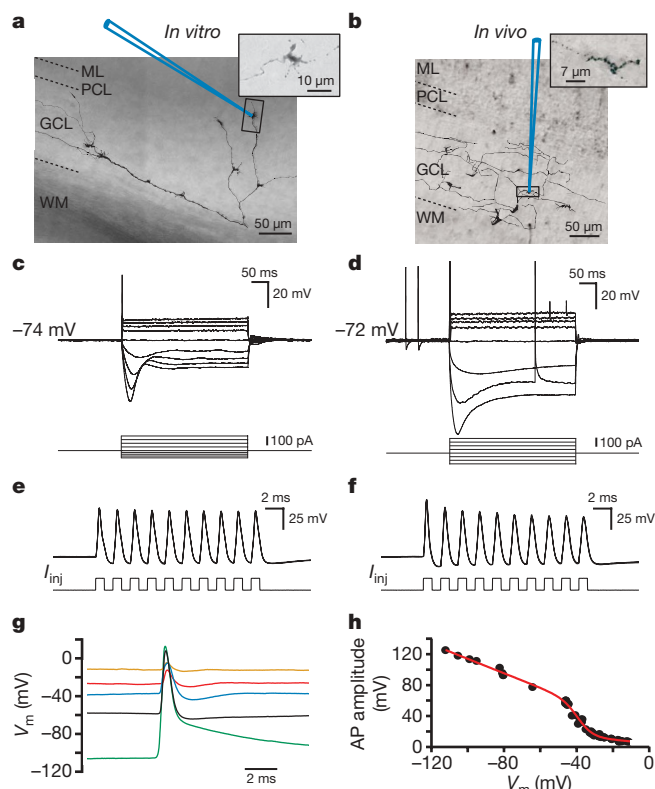


Figure 1 | Properties of mossy fibre boutons *in vitro* and *in vivo*. **a, b**, Whole-cell recordings were made from visually identified mossy fibre boutons in the granule cell layer of rat cerebellar slices by using infrared differential interference contrast microscopy (**a**) or blind-patch recording techniques *in vivo* (**b**). Morphological reconstructions of individual mossy fibres were obtained by biocytin labelling through the recording electrode. The schematic recording pipettes indicate the locations of the mossy fibre bouton recordings (*in vivo*: 549 μ m from the pial surface). ML, molecular layer; PCL, Purkinje cell layer; GCL, granule cell layer; WM, white matter. Insets: fine structure of single 'mossy' ramifications. **c, d**, Mossy fibre boutons *in vitro* (**c**) and *in vivo* (**d**) show outward rectification and membrane potential sag in response to current injection. The occurrence of spontaneous action potentials *in vivo* is not affected by changes in membrane potential. **e, f**, Mossy fibre boutons can be driven to fire action potentials at extremely high frequencies by means of pulsed current injection (1 nA at 500 Hz); *in vitro* (**e**) $V_m = -58$ mV, *in vivo* (**f**) $V_m = -72$ mV, three consecutive traces. **g**, Representative spontaneous action potentials recorded at different membrane potentials *in vivo* (black trace at resting V_m). **h**, Relationship between spontaneous action potential amplitude and membrane potential (with the use of different levels of holding current) for a single mossy fibre bouton *in vivo*. The fit is a sigmoid function multiplied by a linear function to represent Na^+ channel availability and driving force, respectively. **a, c** and **e** were from the same recordings, as were **d, f** and **h**.

with those recorded *in vivo* (Fig. 3). The average amplitudes and paired-pulse ratios of EPSCs *in vivo* fell between those recorded in 1.2 and 2 mM $[Ca^{2+}]_e$ *in vitro* (Fig. 3), suggesting that the release probability *in vivo* was between those obtained in these two *in vitro* conditions.

Given that the instantaneous frequency of presynaptic action potentials can exceed 700 Hz (Fig. 2b), we tested whether mossy fibre boutons can release transmitter at such high frequencies. Unitary mossy fibre EPSCs could reliably follow presynaptic stimulation at extremely high rates, up to 800 Hz for the first two stimuli and up to 500 Hz for the fifth stimulus (Fig. 4a, b). This suggests that single mossy fibre boutons can release transmitter at frequencies comparable to the maximal frequency of presynaptic action potentials and EPSCs observed *in vivo*. Similar to the result for paired-pulse depression (Fig. 3), synaptic depression during high-frequency trains in 1.2 and 2 mM $[Ca^{2+}]_e$ *in vitro* was comparable to that of sensory-evoked EPSCs *in vivo* (Fig. 4c). Despite substantial depression of peak amplitudes during high-frequency trains, the net charge transfer at the mossy fibre–granule cell synapse was affected remarkably little, with only about 30% depression observed at 500 Hz (Fig. 4d). The robustness of transmission at high frequencies was ensured in part by summation of the tails of EPSCs at high frequencies (Fig. 4e), most probably as a result of glutamate spillover from neighbouring synaptic contacts¹⁶. Consistent with this idea was the observation that the rise time of EPSCs and the proportion of slow-rising spillover EPSCs increased during both high-frequency stimulus-evoked EPSC trains *in vitro* and sensory-evoked EPSC bursts *in vivo* (Supplementary Fig. 5). These results demonstrate that a single mossy fibre bouton is capable of providing the rapid bursts of synaptic input to a granule cell observed after sensory stimulation.

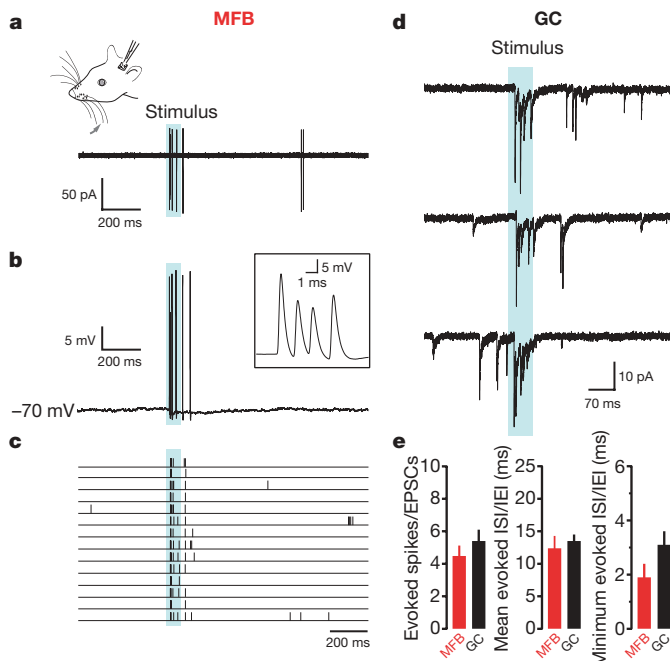


Figure 2 | Sensory-evoked spiking in mossy fibre boutons and EPSCs in granule cells *in vivo*. **a, b**, Cell-attached (**a**) and subsequent whole-cell (**b**) recording from a single mossy fibre bouton during stimulation with air puff (blue shaded area) of the upper lip area and whiskers. Inset: close-up of the high-frequency action potential burst evoked by sensory stimulation. Instantaneous spike frequencies were 658, 735 and 543 Hz, respectively. **c**, Raster plot of sensory-evoked action potentials (14 consecutive trials). **d**, EPSC bursts evoked by sensory stimulation recorded from a granule cell held at -70 mV (three consecutive trials). **e**, Number of presynaptic spikes and postsynaptic EPSCs and mean and minimum ISIs and IEIs evoked in mossy fibre boutons and granule cells by sensory stimulation ($n = 3$ and $n = 14$, respectively; $P > 0.05$). Even when correcting for synaptic failures (from Fig. 4), these values were not significantly different (see Methods).

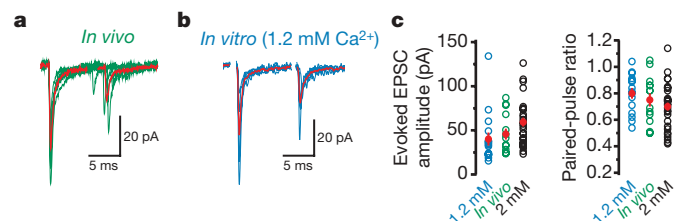


Figure 3 | Synaptic dynamics at the mossy fibre-granule cell synapse *in vivo* and *in vitro*. **a**, Sample EPSC traces evoked by whisker stimulation *in vivo*, aligned to the onset of the first EPSCs. Red traces display the peak-aligned average of the individual trials shown. **b**, Sample EPSC traces evoked by minimal stimulation *in vitro* in 1.2 mM $[Ca^{2+}]_e$. Red traces display the average of the individual trials shown; stimulus artefacts were removed for clarity. **c**, EPSC amplitudes and paired-pulse ratios of experiments *in vivo* (green, $n = 14$) and *in vitro* (1.2 mM $[Ca^{2+}]_e$, blue, $n = 16$; 2 mM $[Ca^{2+}]_e$, black, $n = 28$). The red symbols show means \pm s.e.m. $V_{hold} = -70$ mV in **a** and **b**.

To test whether bursts of synaptic input provided by a single mossy fibre can trigger action potentials in granule cells, we stimulated single mossy fibre inputs (Supplementary Fig. 4) using patterns recorded from mossy fibre boutons *in vivo* (Fig. 5b), or using a regular stimulus pattern (five stimuli at 100 Hz) and recorded the resulting postsynaptic EPSPs and action potentials from postsynaptic granule cells *in vitro*. As the resting membrane potential of granule cells is variable *in vivo*³, we measured the spiking output in response to the stimulus over a range of membrane potentials (Fig. 5a). Granule cells responded with bursts of spikes similar to that evoked *in vivo* with sensory stimulation³, regardless of the extracellular Ca^{2+} concentration or the pattern of presynaptic burst activity (Fig. 5c), confirming that a burst of spikes can be triggered in granule cells by means of a single mossy fibre input.

We have made intracellular recordings from nerve terminals in the intact mammalian brain. Previous recordings *in vitro* have shown that boutons from hippocampal mossy fibres^{6,17}, basket cells¹⁸ and

the calyx of Held¹⁹ show qualitatively similar excitabilities, in particular strong outward rectification. Our results further show that mossy fibre boutons *in vivo* are capable of extremely high maximal firing rates, and that such high firing rates are triggered by sensory stimulation. The sensory-evoked burst of spikes observed in mossy fibre boutons is consistent with rapid burst firing recorded from the somata of neurons that form the mossy fibres in the trigeminal nucleus²⁰, revealing that these high-frequency bursts are reliably transmitted from the soma to the axon terminals many millimetres distant. Our findings suggest that the release properties of mossy fibre boutons are matched to their high firing rates, and robust synaptic charge transfer is achievable at 500 Hz. The high fidelity of mossy fibre transmission is a consequence of several features of this synapse, including the multiple morphological contacts made by a mossy fibre with each granule cell²¹, the rapid recovery of each release site from synaptic release²², and the increasing contribution of glutamate spillover¹⁶ at high frequencies.

The prevailing view of transmission at the relay from mossy fibre to granule cell is that activity in multiple mossy fibres is required to drive spike output^{23–26}. Our findings provide direct support for a fundamentally different mode of operation of this relay, in which the sensory-evoked spiking observed in granule cells³ can arise from a burst of spikes in a single mossy fibre, in an analogous manner to the ‘detonator’ function proposed for mossy fibres in the hippocampus^{27,28}. Although integration of multiple mossy fibre inputs is likely to occur under some circumstances^{23–26}, our findings show that it is not a prerequisite for sensory activation of granule cells *in vivo*, consistent with Marr’s proposal²⁵ that under conditions of reduced input from across a population of mossy fibres, granule cell output can be driven by a single presynaptic mossy fibre. Given that bursts of EPSCs are required to trigger spike output from granule cells *in vivo*³, such an arrangement is ideally suited for the transfer of sensory information coded by a single sensory modality with the maximal signal-to-noise ratio. Such a single-fibre relay also provides the ultimate sensitivity to sensory input, yet it can reject spontaneous

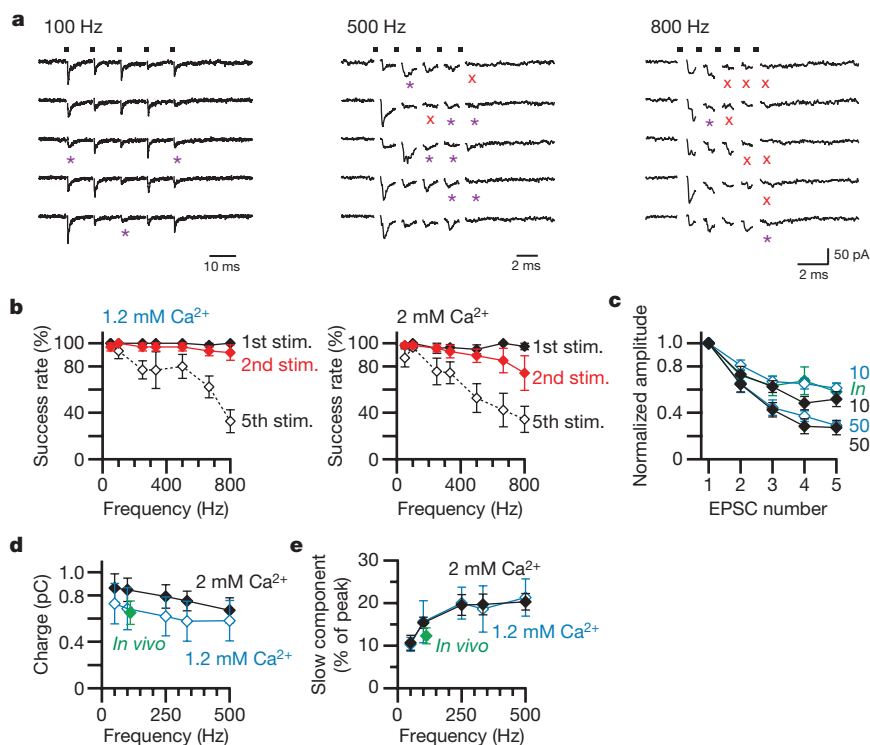


Figure 4 | High-fidelity synaptic transmission at the mossy fibre-granule cell synapse *in vivo* and *in vitro*.

a, Sample EPSC traces evoked by trains of five stimuli at various frequencies *in vitro* in 1.2 mM $[Ca^{2+}]_e$. Five consecutive trials are shown. The dots at the top indicate the timing of the stimuli, the red crosses indicate failures of transmission and the purple asterisks denote slow-rising ‘spillover’ EPSCs. **b**, The probability of success (non-failure) for the first, second and fifth stimuli (stim.) at various frequencies (50–800 Hz). Data were obtained *in vitro* in 1.2 mM $[Ca^{2+}]_e$ (left, $n = 6$) and 2 mM $[Ca^{2+}]_e$ (right, $n = 7–11$).

c, Synaptic depression of EPSCs during trains of five stimuli at 100 and 500 Hz *in vitro* and sensory-evoked EPSCs *in vivo*. Pooled data from 11 cells *in vitro* in 2 mM $[Ca^{2+}]_e$ (filled black symbols), six cells *in vitro* in 1.2 mM $[Ca^{2+}]_e$ (open blue symbols) and 14 cells *in vivo* (filled green symbols).

d, Total EPSC charge transferred by five stimuli at various frequencies *in vitro* in 2 mM $[Ca^{2+}]_e$ ($n = 11$, filled black symbols) and in 1.2 mM $[Ca^{2+}]_e$ ($n = 6$, open blue symbols). Total charge of sensory-evoked EPSCs *in vivo* ($n = 14$, filled green symbol; horizontal error bars are smaller than the symbol) is plotted for the average frequency. **e**, The amplitudes of the slow-current component measured at 10 ms after the last (fifth) stimulus were normalized by the amplitude of the first EPSC. Pooled *in vitro* data in 2 mM $[Ca^{2+}]_e$ (filled black symbols, $n = 9–11$) and in 1.2 mM $[Ca^{2+}]_e$ (open blue symbols, $n = 6$) and *in vivo* data (filled green symbol, $n = 14$). Results are shown as means \pm s.e.m.

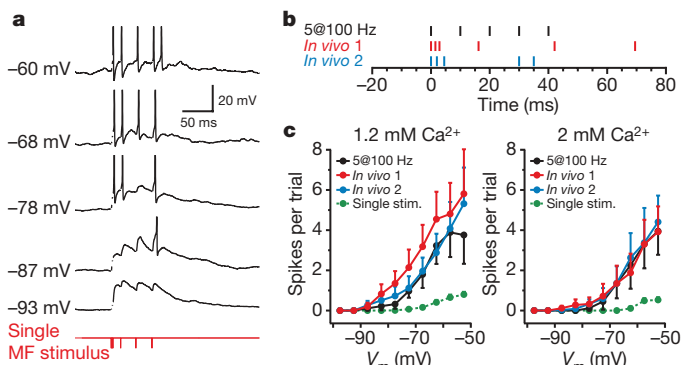


Figure 5 | Input from a single mossy fibre reliably drives granule cell firing. **a**, Stimulation of a single mossy fibre with a sensory-evoked stimulus pattern recorded *in vivo* (labelled 'In vivo 1' in **b**) triggers bursts of action potentials in a granule cell *in vitro* (in 1.2 mM Ca^{2+}). Several sweeps at different membrane potentials (set by adjusting holding current) are shown (same cell as in Supplementary Fig. 4). Spikes are truncated and stimulus artefacts have been removed for clarity. **b**, Schematic representation of three different stimulation patterns used in **c** to activate single mossy fibre inputs (*in vivo* 1 and *in vivo* 2 were taken from different mossy fibre bouton recordings *in vivo*). **c**, Pooled data showing the number of action potentials triggered at different membrane potentials in 1.2 mM Ca^{2+} (left) and 2 mM Ca^{2+} (right).

synaptic input³ and remains modifiable because the number and timing of granule cell output spikes can be regulated by inhibition^{3,29}. The large synaptic divergence of single mossy fibre boutons²¹, and the multiple collaterals shown by each mossy fibre², suggest that a sensory-evoked burst in a single mossy fibre may lead to the activation of a substantial number of neighbouring granule cells. Given that coincident activation of multiple granule cells is required for reliable activation of the downstream Purkinje cells³⁰, this arrangement thus solves the problem of generating synchrony in a population of granule cells with sparse afferent input.

METHODS SUMMARY

In vivo patch-clamp recordings were made from mossy fibre boutons and granule cells in folia Crus I and IIa of the cerebellar cortex of freely breathing 18–27-day-old Sprague–Dawley rats anaesthetized with urethane or with a ketamine/xylazine mixture as described previously³. Sensory responses were evoked by a brief air puff delivered to the ipsilateral whiskers or perioral surface³. Patch-clamp recordings from mossy fibre boutons and granule cells *in vitro* were made at 35–36 °C in cerebellar slices (200 μ m thick) prepared with standard techniques¹⁷. Mossy fibre boutons were revealed by infrared differential interference contrast microscopy, with identification confirmed by biocytin staining after each experiment. For both *in vivo* and *in vitro* experiments, patch pipettes (6–9 M Ω for bouton recordings, and 5–8 M Ω for granule cell recordings) were filled with a potassium methanesulphonate-based internal solution. Data are given as means \pm s.e.m.

Full Methods and any associated references are available in the online version of the paper at www.nature.com/nature.

Received 23 May; accepted 11 October 2007.

- Ramón y Cajal, S. *La Textura del Sistema Nervioso del Hombre y los Vertebrados* (Moya, Madrid, 1904).
- Palay, S. L. & Chan-Palay, V. *Cerebellar Cortex—Cytology and Organization* (Springer, Berlin, 1974).
- Chaderton, P., Margrie, T. W. & Häusser, M. Integration of quanta in cerebellar granule cells during sensory processing. *Nature* **428**, 856–860 (2004).
- Holtzman, T., Rajapaksa, T., Mostofi, A. & Edgley, S. A. Different responses of rat cerebellar Purkinje cells and Golgi cells evoked by widespread convergent sensory inputs. *J. Physiol. (Lond.)* **574**, 491–507 (2006).
- Simpson, J. I., Hulscher, H. C., Sabel-Goedknegt, E. & Ruigrok, T. J. Between in and out: linking morphology and physiology of cerebellar cortical interneurons. *Prog. Brain Res.* **148**, 329–340 (2005).

- Engel, D. & Jonas, P. Presynaptic action potential amplification by voltage-gated Na^+ channels in hippocampal mossy fiber boutons. *Neuron* **45**, 405–417 (2005).
- Hodgkin, A. L. & Huxley, A. F. A quantitative description of membrane current and its application to conduction and excitation in nerve. *J. Physiol. (Lond.)* **117**, 500–544 (1952).
- Eccles, J. C., Faber, D. S., Murphy, J. T., Sabah, N. H. & Taborikova, H. Afferent volleys in limb nerves influencing impulse discharges in cerebellar cortex. I. In mossy fibers and granule cells. *Exp. Brain Res.* **13**, 15–35 (1971).
- van Kan, P. L., Gibson, A. R. & Houk, J. C. Movement-related inputs to intermediate cerebellum of the monkey. *J. Neurophysiol.* **69**, 74–94 (1993).
- Garwicz, M., Jörntell, H. & Ekerot, C. F. Cutaneous receptive fields and topography of mossy fibres and climbing fibres projecting to cat cerebellar C3 zone. *J. Physiol. (Lond.)* **512**, 277–293 (1998).
- Lisberger, S. G. & Fuchs, A. F. Role of primate flocculus during rapid behavioral modification of vestibuloocular reflex. II. Mossy fiber firing patterns during horizontal head rotation and eye movement. *J. Neurophysiol.* **41**, 764–777 (1978).
- Morissette, J. & Bower, J. M. Contribution of somatosensory cortex to responses in the rat cerebellar granule cell layer following peripheral tactile stimulation. *Exp. Brain Res.* **109**, 240–250 (1996).
- Silver, R. A., Cull-Candy, S. G. & Takahashi, T. Non-NMDA glutamate receptor occupancy and open probability at a rat cerebellar synapse with single and multiple release sites. *J. Physiol. (Lond.)* **494**, 231–250 (1996).
- Silver, I. A. & Erecinska, M. Intracellular and extracellular changes of $[Ca^{2+}]$ in hypoxia and ischemia in rat brain *in vivo*. *J. Gen. Physiol.* **95**, 837–866 (1990).
- Kristian, T. & Siesjö, B. K. Calcium in ischemic cell death. *Stroke* **29**, 705–718 (1998).
- DiGregorio, D. A., Nusser, Z. & Silver, R. A. Spillover of glutamate onto synaptic AMPA receptors enhances fast transmission at a cerebellar synapse. *Neuron* **35**, 521–533 (2002).
- Geiger, J. R. P. & Jonas, P. Dynamic control of presynaptic Ca^{2+} inflow by fast-inactivating K^+ channels in hippocampal mossy fiber boutons. *Neuron* **28**, 927–939 (2000).
- Southan, A. P., Morris, N. P., Stephens, G. J. & Robertson, B. Hyperpolarization-activated currents in presynaptic terminals of mouse cerebellar basket cells. *J. Physiol. (Lond.)* **526**, 91–97 (2000).
- Cuttle, M. F., Rusznák, Z., Wong, A. Y., Owens, S. & Forsythe, I. D. Modulation of a presynaptic hyperpolarization-activated cationic current (I_h) at an excitatory synaptic terminal in the rat auditory brainstem. *J. Physiol. (Lond.)* **534**, 733–744 (2001).
- Jones, L. M., Lee, S., Trageser, J. C., Simons, D. J. & Keller, A. Precise temporal responses in whisker trigeminal neurons. *J. Neurophysiol.* **92**, 665–668 (2004).
- Jakab, R. L. & Hamori, J. Quantitative morphology and synaptology of cerebellar glomeruli in the rat. *Anat. Embryol. (Berl.)* **179**, 81–88 (1988).
- Saviane, C. & Silver, R. A. Fast vesicle reloading and a large pool sustain high bandwidth transmission at a central synapse. *Nature* **439**, 983–987 (2006).
- Albus, J. S. A theory of cerebellar function. *Math. Biosci.* **10**, 25–61 (1971).
- D'Angelo, E., De Filippi, G., Rossi, P. & Taglietti, V. Synaptic excitation of individual rat cerebellar granule cells *in situ*: evidence for the role of NMDA receptors. *J. Physiol. (Lond.)* **484**, 397–413 (1995).
- Marr, D. A theory of cerebellar cortex. *J. Physiol. (Lond.)* **202**, 437–470 (1969).
- Jörntell, H. & Ekerot, C. F. Properties of somatosensory synaptic integration in cerebellar granule cells *in vivo*. *J. Neurosci.* **26**, 11786–11797 (2006).
- McNaughton, B. L. & Morris, R. G. M. Hippocampal synaptic enhancement and information storage within a distributed memory system. *Trends Neurosci.* **10**, 408–415 (1987).
- Henze, D. A., Wittner, L. & Buzsáki, G. Single granule cells reliably discharge targets in the hippocampal CA3 network *in vivo*. *Nature Neurosci.* **5**, 790–795 (2002).
- Maex, R. & De Schutter, E. Synchronization of Golgi and granule cell firing in a detailed network model of the cerebellar granule cell layer. *J. Neurophysiol.* **80**, 2521–2537 (1998).
- Barbour, B. Synaptic currents evoked in Purkinje cells by stimulating individual granule cells. *Neuron* **11**, 759–769 (1993).

Supplementary Information is linked to the online version of the paper at www.nature.com/nature.

Acknowledgements We thank J. Geiger for guidance during the slice experiments; B. Clark, J. Davie, M. Farrant and A. Roth for comments on the manuscript; K. Kitamura, S. Komai and M. Rizzi for help with preliminary experiments; and L. Ramakrishnan and H. Cuntz for help with histology. This work was supported by grants from the European Union, Wellcome Trust and Gatsby Foundation (M.H.), and by a Wellcome Prize Studentship (E.A.R.), a Human Frontier Science Program Long-Term Fellowship (T.I.), a Wellcome Trust Advanced Training Fellowship (I.D.) and a University College London Graduate School Research Scholarship (P.C.).

Author Information Reprints and permissions information is available at www.nature.com/reprints. Correspondence and requests for materials should be addressed to M.H. (m.hausser@ucl.ac.uk).

METHODS

The care and experimental manipulation of animals were conducted in accordance with institutional and national guidelines.

General. Current-clamp and voltage-clamp recordings were made with Multiclamp 700A and 700B amplifiers (Molecular Devices). The internal solution contained (in mM): potassium methanesulphonate 133, KCl 7, HEPES 10, MgATP 2, Na₂ATP 2, Na₂GTP 0.5, EGTA 0.05 (pH 7.2). Biocytin (0.5%) was added for subsequent morphological reconstruction. Data were filtered at 3–10 kHz and acquired at 50 kHz using Axograph software (<http://axographx.com/>) in conjunction with an ITC-18 interface (Instrutech). Seal resistance was always more than 3 GΩ in the cell-attached configuration. Resting membrane potentials (V_m) were measured immediately after formation of the whole-cell configuration ('break-in'). The series resistance for *in vitro* and *in vivo* mossy fibre terminal recordings was $35 \pm 10 \text{ M}\Omega$ ($n = 8$) and $72 \pm 20 \text{ M}\Omega$ ($n = 4$), determined from the passive current response to a voltage step at the end of the recording (see Supplementary Fig. 2). For recordings from granule cells, the series resistance was $32 \pm 3 \text{ M}\Omega$ ($n = 44$) and $33 \pm 2 \text{ M}\Omega$ ($n = 14$) for *in vitro* and *in vivo* recordings, respectively. Capacitive currents recorded from mossy fibre terminals in response to voltage steps were described by a double-exponential function (Supplementary Fig. 2), with the dominant fast component presumably corresponding to the charging of the terminal, and the slower component representing the axon¹⁷. The fast component was used to estimate the capacitance of the terminal.

In vivo recordings. Sprague–Dawley rats (18–27 days old) were anaesthetized with urethane (1.2 g kg^{-1}) or with a ketamine (50 mg kg^{-1})/xylazine (5 mg kg^{-1}) mixture as described previously^{3,31}. Recordings were made more than 400 μm from the pial surface in the granule cell layer. Sensory stimulation was performed with an airpuff (30–70 ms, 60 lb in⁻² (approx. 410 kPa)) timed by a Picospritzer (General Valve) and aimed at the ipsilateral whiskers or perioral surface with a glass tube mounted on a micromanipulator.

In vitro recordings. Recordings from mossy fibre boutons in slices were made with standard techniques³². The external solution contained (in mM): NaCl 125, NaHCO₃ 25, glucose 25, KCl 2.5, NaH₂PO₄ 1.25, CaCl₂ 2, MgCl₂ 1 (pH 7.3 when bubbled with 95% O₂ and 5% CO₂). In some experiments, CaCl₂ concentration was decreased to 1.2 mM as described, because previous reports^{14,15,33} had indicated that $[\text{Ca}^{2+}]_e$ in the cerebrospinal fluid may be somewhat lower than that widely used for *in vitro* slice experiments. The recording chamber was continuously perfused with external solutions and maintained at physiological temperature (35–36 °C). EPSCs were evoked by extracellular stimulation (100 μs, typically 5–15 V) at 0.5 Hz, unless otherwise stated, using a monopolar electrode or a bipolar electrode made from a theta capillary filled with external solution and placed in the granule cell layer, about 50 μm from the recording site. EPSCs from single mossy fibre inputs were identified by their all-or-none appearance when the stimulation strength was gradually increased¹³ (see Supplementary Fig. 4).

Analysis. Data analysis was performed with Axograph and Igor Pro (Wavemetrics). Input resistance and rectification ratio were calculated from the voltage response to symmetrical hyperpolarizing or depolarizing current steps (400 ms; 10–40 pA) from rest, measured at the end of the step. Sag ratio was calculated as the peak divided by the steady-state input resistance from

hyperpolarizing voltage deflections reaching -100 mV . Spike broadening *in vivo* was calculated by normalizing the half-width of the spike following the shortest ISI in the sensory-evoked burst by the half-width of the first spike. Spike broadening *in vitro* was measured with current-injection-evoked spike trains (five at 100 Hz), and the half-width of the fifth spike was normalized by the half-width of the first spike. EPSC traces were digitally low-pass filtered (3 kHz). The latency of sensory-evoked presynaptic action potentials and postsynaptic EPSCs were corrected to account for the temporal delay of the air puff associated with the application system. For stimulus-evoked EPSCs, synaptic responses were categorized as successes when their amplitudes were larger than a threshold (typically about 7 pA), defined as 4.5-fold the standard deviation of the baseline noise. Synaptic charge measurements were made by using averaged traces from which artefacts were removed by linear interpolation between points immediately before and after the artefacts. To identify 'spillover' EPSCs¹⁶ *in vitro* and *in vivo*, events were defined as slow-rising spillover EPSCs if the 20–80% rise time was longer than 1.6-fold the median of the rise-time distribution obtained from the same cell. This cut-off value roughly corresponded to the mean plus four times the standard deviation because the coefficient of variation of the rise-time distribution was typically 0.15 in cells that did not show obvious slow-rising events. These criteria corresponded well to events categorized by eye. Statistical comparisons were made with Student's two-sided paired *t*-test unless otherwise indicated.

The effect of synaptic failures on *in vivo* sensory-evoked EPSCs was evaluated by numerical simulation with the sensory-evoked spiking pattern of *in vivo* mossy fibre boutons (Fig. 2) and the average failure rate estimated from mossy fibre stimulation experiments (Fig. 4b; $1.2 \text{ mM } [\text{Ca}^{2+}]_e$ *in vitro*). For each presynaptic action potential, a failure rate was defined by using a value corresponding to the nearest ISI shown in Fig. 4b. Values from 1,000 random trials were averaged for each cell. As described in the results and in Fig. 2, the number, minimum interval and mean interval of sensory-evoked presynaptic spikes in single boutons were 4.2 ± 0.6 , $1.9 \pm 0.5 \text{ ms}$ and $12.4 \pm 1.7 \text{ ms}$, respectively ($n = 3$). If there are no failures and there is perfectly reliable transmission across the synapse, the corresponding values for postsynaptic sensory-evoked EPSCs should be identical (assuming that only one bouton is involved). Taking into account the failure rate, the number, minimum interval and mean interval of EPSCs were predicted to be 3.9 ± 0.5 , $1.9 \pm 0.5 \text{ ms}$ and $13.0 \pm 1.7 \text{ ms}$, respectively ($n = 3$). These values were similar to the number (5.4 ± 0.7 ; $P = 0.35$), the minimum interval ($3.1 \pm 0.5 \text{ ms}$; $P = 0.27$) and the mean interval ($13.5 \pm 1.0 \text{ ms}$; $P = 0.82$) of actual sensory-evoked EPSCs ($n = 14$, unpaired *t*-test). This result is consistent with our conclusion that the sensory-evoked EPSCs arise from activity in a single mossy fibre.

31. Margrie, T. W., Brecht, M. & Sakmann, B. *In vivo*, low-resistance, whole-cell recordings from neurons in the anaesthetized and awake mammalian brain. *Pflügers Arch.* **444**, 491–498 (2002).
32. Bischofberger, J., Engel, D., Li, L., Geiger, J. R. & Jonas, P. Patch-clamp recording from mossy fiber terminals in hippocampal slices. *Nature Protocols* **1**, 2075–2081 (2006).
33. Leusen, I. Regulation of cerebrospinal fluid composition with reference to breathing. *Physiol. Rev.* **52**, 1–56 (1972).